Chapter 12

Particle-Wall Interactions

12.1 The Lorentz Image

In previous chapters we have considered interactions between particles. We now address another important class of hydrodynamic interaction problems, namely, the influence of nearby walls on the motion of small particles. In many respects, the analysis for particle-wall interactions parallels that for particle-particle interactions. Here again, the method of choice depends on the ratio of two length scales: the particle size and the separation between the particle and wall. When the particle is far away from the wall, a suitably modified form of the method-of-reflections technique is appropriate — as in the previous chapter, the reflections off the wall are conveniently represented by image singularities. This approach has a long history dating back to the works of Lorentz [52] and Faxén [13]. An excellent summary of work up to 1965 on particle-wall interactions by the method of reflections (for particles of arbitrary shape and various wall geometries) may be found in Chapter 7 of Happel and Brenner [27], along with analytical solutions for special geometries (*e.g.*, sphere near a plane). More recent works by Liron and Mochon [51] and Hackborn [25] consider flows produced by Stokeslets and rotlets in channels bounded by two parallel plane walls; these works provide analytic expressions for the Green's function in such geometries and thus form the basis for further numerical work.

For particles and walls near contact, a combination of lubrication and numerical methods is required. The resistance functions for rigid particles and walls in relative motion are singular at touching and, as was the case for interactions between two particles, the singular leading order terms originate from the flow in the gap region, whence lubrication methods apply. Contributions to the higher order, nonsingular terms come from all regions and thus, except for a limited number of fortuitous geometries such as the sphere-plane problem [4, 56], a numerical approach is unavoidable. Also, for particles sliding near a wall, the leading order singular term is only logarithmic (see Chapter 9), and thus higher order terms really are essential for most applications.

For moderate separations, we again require numerical solutions. We will present two such methods in this book. The boundary-multipole collocation

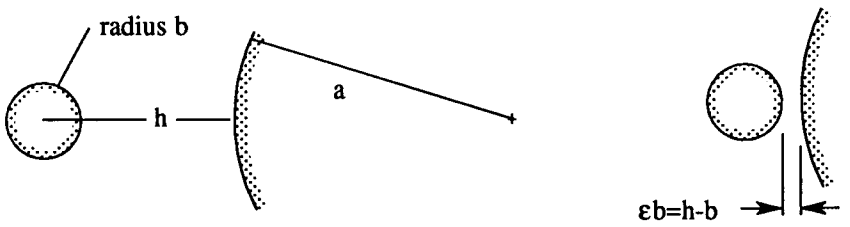

Figure 12.1: Particle-wall interactions: widely-separated and near-contact.

method of the following chapter provides an efficient method for particles of simple shape (for a representative sample, see [19, 20, 31, 65]). For particles and walls of complex shape and many-body problems, all of which lead to large system of equations, we recommend the boundary integral method described in Part IV.

The focus of this chapter will be primarily on the analysis of the image systems of the Stokeslet and other lower order singularities for two pedagogical reasons. These singularities may be used to represent the particle as in Chapter 3, and their images form the basis for the method of reflections. Furthermore, most numerical methods for particulate Stokes involve velocity representations that are distributions of Stokeslets and higher order singularities on or inside the particle. Therefore, given the image system for a Stokeslet near a wall, we have a straightforward generalization of the numerical method to the case of particles near a wall.

12.2 Stokeslet Near a Rigid Wall

Consider the image solution for a point force near a stationary sphere, which we derived in Section 10.2.3. From it, we can obtain the image for the plane wall by increasing the radius a while keeping constant the distance between the singularity and the nearest point on the sphere (see Figure 12.2). We write

$$\frac{R}{a} = 1 + \frac{h}{a} ,$$

and in the limit of small h/a, the image inside the sphere reduce to the following solution:

$$\begin{aligned} \boldsymbol{v}^* &= -(\boldsymbol{F}^{\perp} + \boldsymbol{F}^{\parallel}) \cdot \mathcal{G}(\boldsymbol{x} - \boldsymbol{y}^*) - 2h[(\boldsymbol{F}^{\perp} - \boldsymbol{F}^{\parallel}) \cdot \nabla]\boldsymbol{n} \cdot \mathcal{G}(\boldsymbol{x} - \boldsymbol{y}^*) \\ &\quad + h^2(\boldsymbol{F}^{\perp} - \boldsymbol{F}^{\parallel}) \cdot \nabla^2\mathcal{G}(\boldsymbol{x} - \boldsymbol{y}^*) , \end{aligned} \tag{12.1}$$

where $\boldsymbol{n}$ (pointing into the fluid) is the normal for the plane and $\boldsymbol{y}$ and $\boldsymbol{y}^*$ are the new designations for the singular point $\boldsymbol{x}_2$ and the inverse point $\boldsymbol{x}_2^*$.

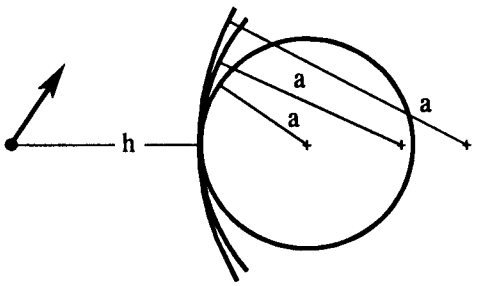

Figure 12.2: Stokeslet-wall interaction from a limiting procedure using large spheres.

Note that $\boldsymbol{y}^*$ is the mirror image of $\boldsymbol{y}$, whence if we choose our coordinate system so that the Stokeslet is on the z-axis and the plane is at $z = 0$, then $\boldsymbol{y}^* = -\boldsymbol{y}$. In contrast to the solution for the sphere, here the image systems for both axisymmetric and transverse cases are degenerate, consisting only of the inverse point, $\boldsymbol{y}^*$. Furthermore, the various singularities possess equal strengths in the axisymmetric ($\boldsymbol{F}^{\parallel}$) and transverse ($\boldsymbol{F}^{\perp}$) cases.[1] We shall exploit these properties presently.

Although Equation 12.1 is a valid expression for the image system (and as we shall see later, quite useful in its own right), we display the following alternate expression in which the geometric parameter h does not appear explicitly:

$$\boldsymbol{v}^* = -(\boldsymbol{\delta} - 2\boldsymbol{nn}) \cdot \boldsymbol{u} - 2\boldsymbol{n} \cdot \boldsymbol{x}\nabla(\boldsymbol{n} \cdot \boldsymbol{u}) + (\boldsymbol{n} \cdot \boldsymbol{x})^2\nabla^2\boldsymbol{u} \ , \tag{12.2}$$

with

$$\boldsymbol{u} = (\boldsymbol{F}^{\perp} - \boldsymbol{F}^{\parallel}) \cdot \mathcal{G}(\boldsymbol{x} - \boldsymbol{y}^*) \ . \tag{12.3}$$

Equation 12.2 is the image solution of Lorentz [52] and the equivalence of Equations 12.1 and 12.2 is readily demonstrated.

According to Equation 12.3, $\boldsymbol{u}$ is the field generated by a Stokeslet located at the image point. Since this image Stokeslet ($\boldsymbol{F}^{\perp} - \boldsymbol{F}^{\parallel}$) is the mirror reflection of the original (see Figure 12.3), its vector field, $\boldsymbol{u}$, is also obtained by mirror reflection of $\boldsymbol{F} \cdot \mathcal{G}(\boldsymbol{x} - \boldsymbol{y})$, as can be verified directly. The mirror reflection operation may be defined formally by introducing the operator $\mathcal{M}$ defined by[2] $\boldsymbol{u} = \mathcal{M}\boldsymbol{v}$, with

$$\boldsymbol{u}(x, y, z) = \mathcal{M}(\boldsymbol{v}) = (\boldsymbol{\delta} - 2\boldsymbol{e}_3\boldsymbol{e}_3) \cdot \boldsymbol{v}(x, y, -z) \ , \tag{12.4}$$

for a plane wall coincident with the xy-plane.

[1] The $\parallel$ and $\perp$ designations are relative to the symmetry axis. Some authors reverse this notation for the plane, *i.e.*, $\perp$ designates orientation normal to the plane.

[2] Lee [47] denotes this operation by an asterisk and the Lorentz operation with a caret.

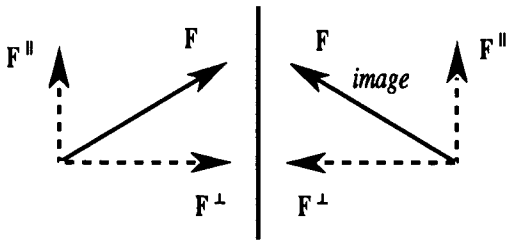

Figure 12.3: The mirror reflection operation for the Stokeslet field.

Going back to Equation 12.2, we see that the image field for the Stokeslet may be written as

$$v^* = \hat{u} \ , \qquad u = \mathcal{M}(v) \ , \tag{12.5}$$

where the "hat" operator is defined by

$$\hat{u} = -(\delta - 2nn) \cdot u - 2z\nabla u_z + z^2\nabla^2 u \ . \tag{12.6}$$

Equations 12.5 and 12.6 transform the Stokeslet into its image solution. By the linearity of the Stokes equation (or direct verification), we see that the *Lorentz reflection* for the wall, defined by Equations 12.5 and 12.6, is in fact a general result that applies to any solution of the Stokes equations.

The mirror reflection and Lorentz ("hat") operators share two important properties. First, if v is a solution of the Stokes equation, then $\mathcal{M}(v(x,y,z))$ and $\hat{v}$ are also solutions of the Stokes equations. The associated pressure fields are

$$\mathcal{M}(p(x,y,z)) = p(x,y,-z)$$

and

$$\hat{p} = p + 2z\frac{\partial p}{\partial z} - 4\frac{\partial v_z}{\partial z} \ .$$

Second, the operators commute, *i.e.*, $\mathcal{M}(\hat{v}) = \hat{u}$ where $u = \mathcal{M}(v)$.

In the following example, we use the preceding result to calculate the mobility of a sphere translating near a plane wall.

Example 12.1 Mobility of a Sphere Far Away from a Plane Wall. Consider a torque-free sphere near a plane wall. We will derive expressions for the translational and rotational velocities by the method of reflections, when the sphere is subject to a net external force F^{ext}.

We center the sphere of radius b at a distance h from the plane. We will correct Stokes' law to $O(h^{-3})$ by incorporating the contributions from the images for the Stokeslet and degenerate quadrupole. The velocity field due to an

isolated, translating sphere, subject to an external force $\boldsymbol{F}^{ext}$, in a quiescent fluid is

$$\boldsymbol{v}_1 = \boldsymbol{F}^{ext} \cdot (1 + \frac{b^2}{6}\nabla^2)\frac{\mathcal{G}(\boldsymbol{x}-\boldsymbol{y})}{(8\pi\mu)} ,$$

with $\boldsymbol{F}^{ext} = 6\pi\mu b\boldsymbol{U}$ and $\boldsymbol{y} = h\boldsymbol{n}$.

At the first reflection on the wall (surface 2), $\boldsymbol{v}_{12}$ is simply the image system for the Stokeslet and the degenerate quadrupole. If we split the external force into components along and transverse to the plane normal, $\boldsymbol{F}^{ext} = \boldsymbol{F}^{\parallel} + \boldsymbol{F}^{\perp}$, then the image systems for the Stokeslet and degenerate Stokes quadrupole coefficient $\boldsymbol{Q} = (b^2/6)\boldsymbol{F}^{ext}$ may be written as

$$\begin{aligned}
\boldsymbol{v}_{12} \;=\; & -(\boldsymbol{F}^{\parallel} + \boldsymbol{F}^{\perp}) \cdot \frac{\mathcal{G}(\boldsymbol{x}-\boldsymbol{y}^*)}{8\pi\mu} \\
& + 2h[(\boldsymbol{F}^{\parallel} - \boldsymbol{F}^{\perp}) \cdot \nabla]\boldsymbol{n} \cdot \frac{\mathcal{G}(\boldsymbol{x}-\boldsymbol{y}^*)}{8\pi\mu} \\
& - h^2(\boldsymbol{F}^{\parallel} - \boldsymbol{F}^{\perp}) \cdot \nabla^2\frac{\mathcal{G}(\boldsymbol{x}-\boldsymbol{y}^*)}{8\pi\mu} \\
& + 4(\boldsymbol{n}\cdot\nabla)^2(\boldsymbol{Q}^{\parallel} + \boldsymbol{Q}^{\perp}) \cdot \frac{\mathcal{G}(\boldsymbol{x}-\boldsymbol{y}^*)}{8\pi\mu} \\
& - 2h(\boldsymbol{n}\cdot\nabla)(\boldsymbol{Q}^{\parallel} - \boldsymbol{Q}^{\perp}) \cdot \frac{\mathcal{G}(\boldsymbol{x}-\boldsymbol{y}^*)}{8\pi\mu} \\
& - (3\boldsymbol{Q}^{\parallel} - \boldsymbol{Q}^{\perp}) \cdot \nabla^2\frac{\mathcal{G}(\boldsymbol{x}-\boldsymbol{y}^*)}{8\pi\mu} \\
& - 8(\boldsymbol{n}\cdot\nabla)(\boldsymbol{Q}^{\perp}\times\boldsymbol{n}) \times \nabla\frac{1}{8\pi\mu|\boldsymbol{x}-\boldsymbol{y}^*|} ,
\end{aligned}$$

with $\boldsymbol{y}^* = -h\boldsymbol{n}$.

The second reflection is at the sphere, and here the translational and rotational velocities are obtained by applying the Faxén laws for a force-free and torque-free sphere. Note that we do not need the Faxén correction for the image field of the degenerate quadrupole, since this image is already $O(h^{-3})$. Thus the terms of interest are

$$\begin{aligned}
\boldsymbol{v}_{12}|_{x=y} \;=\; & -\left(\frac{3}{2h}\right)\frac{\boldsymbol{F}^{\parallel}}{8\pi\mu} - \left(\frac{3}{4h}\right)\frac{\boldsymbol{F}^{\perp}}{8\pi\mu} \\
& + \left(\frac{2}{h^3}\right)\frac{\boldsymbol{Q}^{\parallel}}{8\pi\mu} + \left(\frac{1}{2h^3}\right)\frac{\boldsymbol{Q}^{\perp}}{8\pi\mu}
\end{aligned}$$

and

$$\nabla^2\boldsymbol{v}_{12}|_{x=y} \;=\; \left(\frac{2}{h^3}\right)\frac{\boldsymbol{F}^{\parallel}}{8\pi\mu} + \left(\frac{1}{2h^3}\right)\frac{\boldsymbol{F}^{\perp}}{8\pi\mu} .$$

The equality between the $O(h^{-3})$ coefficients in $\boldsymbol{v}_{12}$ and $\nabla^2\boldsymbol{v}_{12}$ is a consequence of the Lorentz reciprocal theorem (see Exercise 12.4). The translational velocity

follows immediately as

$$\begin{aligned} 6\pi\mu b\boldsymbol{U} &= \boldsymbol{F}^{ext} + 6\pi\mu b(1 + \frac{b^2}{6}\nabla^2)\boldsymbol{v}_{12}(\boldsymbol{x})|_{x=y} \\ &= \left[1 - \frac{9}{8}\frac{b}{h} + \frac{1}{2}\left(\frac{b}{h}\right)^3\right]\boldsymbol{F}^{\parallel} + \left[1 - \frac{9}{16}\frac{b}{h} + \frac{1}{8}\left(\frac{b}{h}\right)^3\right]\boldsymbol{F}^{\perp} , \end{aligned}$$

with an error of $O((b/h)^5)$.

The rotational velocity is obtained in an analogous fashion, by applying the Faxén law to the image fields. The vorticity of the image for the Stokeslet is identically zero at $\boldsymbol{y}$, so the leading term for the rotational velocity comes from the image of the degenerate quadrupole. Thus, at the second reflection,

$$\begin{aligned} \boldsymbol{\omega}^{(2)} &= \frac{1}{2}\nabla \times \boldsymbol{v}_{12}(\boldsymbol{x})|_{x=y} \\ &= -\frac{3}{4h^4}\frac{\boldsymbol{Q}^{\perp}}{8\pi\mu} \times \boldsymbol{n} \\ &= -\frac{b^2}{8h^4}\frac{\boldsymbol{F}^{\perp} \times \boldsymbol{n}}{8\pi\mu} . \end{aligned}$$

Thus a torque-free sphere dragged near a wall by an external force rotates weakly in a rolling motion.

The fourth reflection contributes the next term for the rotational velocity, and this contribution comes from the vorticity field of the image of the stresslet,

$$\boldsymbol{S} = \frac{5b^3}{16h^2}(\boldsymbol{F}^{\perp}\boldsymbol{n} + \boldsymbol{n}\boldsymbol{F}^{\perp}) , \tag{12.7}$$

induced at the second reflection. This stresslet is of type $m = 1$ defined in Chapter 10 in the discussion on image solutions for the sphere. If we take the limit of small h/a, then the vorticity of this image system becomes

$$\begin{aligned} \nabla \times \Big[&(\boldsymbol{S} \cdot \nabla) \cdot \frac{\mathcal{G}(\boldsymbol{x} - \boldsymbol{y}^*)}{8\pi\mu} + 2h(\boldsymbol{n} \cdot \nabla)(\boldsymbol{S} \cdot \nabla) \cdot \frac{\mathcal{G}(\boldsymbol{x} - \boldsymbol{y}^*)}{8\pi\mu} \\ &+ 4h(\boldsymbol{n} \cdot \nabla)[(\boldsymbol{S} \cdot \boldsymbol{n}) \times \boldsymbol{n}] \times \nabla \frac{1}{8\pi\mu|\boldsymbol{x} - \boldsymbol{y}^*|}\Big] , \end{aligned}$$

which at $\boldsymbol{x} = \boldsymbol{y}$, with Equation 12.7 for the stresslet, reduces to

$$\frac{15b^3}{64h^5}\frac{\boldsymbol{F}^{\perp} \times \boldsymbol{n}}{8\pi\mu} .$$

Combining the second and fourth reflection contributions, we obtain

$$\boldsymbol{\omega} = -\frac{b^2}{8h^4}\left(1 - \frac{15}{16}\frac{b}{h}\right)\frac{\boldsymbol{F}^{\perp} \times \boldsymbol{n}}{8\pi\mu} .$$

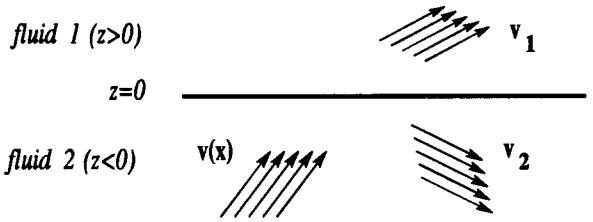

Figure 12.4: Geometry for the reflection from a fluid-fluid interface.

We may replace $\boldsymbol{F}^{\perp}$ with the more readily observable translational velocity, and our expression for the rotational velocity now becomes

$$\begin{aligned}\boldsymbol{\omega} &= -\frac{b^2}{8h^4}\left(1-\frac{15}{16}\frac{b}{h}\right)\frac{3b}{4}\left(1-\frac{9}{16}\frac{b}{h}\right)^{-1}\boldsymbol{U}\times\boldsymbol{n} \\ &= -\frac{3}{32b}\left(\frac{b}{h}\right)^4\left(1-\frac{3}{8}\frac{b}{h}\right)\boldsymbol{U}\times\boldsymbol{n}\,,\end{aligned}$$

a result given in Faxén's thesis and cited in [27]. ◊

12.3 A Drop Near a Fluid-Fluid Interface

In the previous section, we described Lorentz' reflection for a rigid plane wall. The generalization to a planar fluid-fluid interface has been derived by Lee *et al.* [47]. We place the fluid-fluid interface on the plane $z = 0$, and designate the region $z > 0$ as "fluid 1" and $z < 0$ as "fluid 2," as shown in Figure 12.4. We denote the viscosity ratio as $\lambda = \mu_1/\mu_2$.

Consider a velocity field $\boldsymbol{v}$ in fluid 2 that satisfies the Stokes equations. Then the following velocity fields in fluids 1 and 2,

$$\begin{aligned}\boldsymbol{v}_1 &= \frac{1}{1+\lambda}(\boldsymbol{v}-\widehat{\boldsymbol{v}}) \\ \boldsymbol{v}_2 &= (\boldsymbol{v}+\mathcal{M}(\boldsymbol{v}))-\frac{\lambda}{1+\lambda}\mathcal{M}(\boldsymbol{v}+\widehat{\boldsymbol{v}})\,,\end{aligned}$$

with the pressure fields,

$$\begin{aligned}p_1 &= \frac{\lambda}{1+\lambda}(p-\widehat{p}) \\ p_2 &= (p+\mathcal{M}(p))-\frac{\lambda}{1+\lambda}\mathcal{M}(p+\widehat{p})\,,\end{aligned}$$

satisfy the Stokes equations in the two regions, as well as the boundary conditions at the fluid-fluid interface:

$$\begin{aligned} \boldsymbol{n}\cdot\boldsymbol{v}_1 &= 0 \\ \boldsymbol{n}\cdot(\boldsymbol{v}+\boldsymbol{v}_2) &= 0 \\ (\boldsymbol{\delta}-\boldsymbol{nn})\cdot\boldsymbol{v}_1 &= (\boldsymbol{\delta}-\boldsymbol{nn})\cdot(\boldsymbol{v}+\boldsymbol{v}_2) \\ (\boldsymbol{\delta}-\boldsymbol{nn})\cdot(\boldsymbol{\sigma}_1\cdot\boldsymbol{n}) &= (\boldsymbol{\delta}-\boldsymbol{nn})\cdot(\boldsymbol{\sigma}_2\cdot\boldsymbol{n})\ . \end{aligned}$$

We refer to this result as *Lee's reflection lemma.* Note that in the limit of the rigid wall, $\lambda \to \infty$, $\boldsymbol{v}_2$ is the Lorentz reflection from the rigid wall, as required.

Although this lemma can be verified directly by substitution, an easier proof follows from the results of Section 10.2.4 concerning the image solution for a point force near a stationary spherical drop. Analogous to the derivation of the Lorentz reflection principle for the rigid wall, we increase the drop radius a while keeping constant the distance h between the singularity and the nearest point on the sphere. It can be shown that all line integrals appearing in the image field vanish in the limit of small h/a at least as fast as $(h/a)\log(h/a)$ (see Exercise 12.1). But all terms nonlinear in $\Lambda = \lambda/(1+\lambda)$ appear with the line integrals, so *the image of a Stokeslet near a fluid-fluid interface must be a linear function in* Λ of the form

$$\Lambda\boldsymbol{v}^w + (1-\Lambda)\boldsymbol{v}^b\ ,$$

where $\boldsymbol{v}^w$ is the image field for the rigid wall, as described in Section 12.2, and $\boldsymbol{v}^b$ is the image field for a shear-free interface (the limit obtained from a large bubble). The latter is given by the expression,

$$\boldsymbol{v}^b = (\boldsymbol{F}^{\perp} - \boldsymbol{F}^{\parallel})\cdot\mathcal{G}(\boldsymbol{x}-\boldsymbol{y}^*)\ . \tag{12.8}$$

According to this equation, the image of a Stokeslet in fluid 2 when the interface is shear-free is simply its mirror reflection in (inviscid) fluid 1, which of course could have been derived directly by symmetry arguments that apply to any Stokes velocity field in fluid 2.

We now put together the results for the rigid wall and shear-free interface; *the reflection at the fluid-fluid interface is a linear combination (in* Λ*) of the results for a rigid plane wall and a shear-free surface, with the latter obtained simply by a mirror reflection*, and this is precisely the restatement of *Lee's Reflection Lemma.*

The lemma may be used to derive analytical expressions for the resistance and mobility functions for a particle or drop far away from a fluid-fluid interface, in a manner reminiscent of the preceding section for the rigid wall. Examples may be found in the literature ranging from spheres to slender bodies [47, 66, 67]. Furthermore, it can also be used as the basis of numerical schemes, with Stokeslets and other singularities distributed on the particle and drops, and the interface treated with the appropriate images [48].

For large but finite surface tensions, the fluid-fluid interface must deform because of particle motion. The effect of small deviations in the shape of the

interface can be analyzed by linearization of the boundary condition at the interface, and new effective boundary conditions are obtained. These, however, can be treated exactly by the Lorentz reciprocal theorem so that the first effects of interfacial deformation can be handled entirely within the context of particulate motion near a planar interface (see Yang and Leal [68]).

Exercises

Exercise 12.1 Images for a Stokeslet Near a Rigid Plane Wall and for a Stokeslet Near a Planar Fluid-Fluid Interface.
Derive the images for a Stokeslet near a rigid wall and for a Stokeslet near a fluid-fluid interface, from the image solutions for a Stokeslet at a distance h from a sphere of radius a, by taking the limit of small h/a. Show that the line distributions (the terms nonlinear in Λ) in the image for a spherical drop vanish in the limit of small h/a.

Exercise 12.2 The Lorentz Image for a Stokeslet Near a Rigid Plane Wall.
Show that the image for a Stokeslet near a rigid plane wall derived by the above limiting procedure is identical to that of Lorentz, Equation 12.2.
Comment: The rigid wall has a dissipative effect on the flow produced by the Stokeslet; we should expect a much weaker flow in the far field, in comparison to the flow produced by a Stokeslet in unbounded flow. For a Stokeslet in the channel bounded by *two* plane walls, the far field is yet weaker. For example, the paper by Liron and Mochon [51] shows that the far field of a Stokeslet parallel to the plane walls is that of a two-dimensional source-sink doublet, *i.e.*,

$$v_i \sim \frac{D_j}{2\pi\mu}\left(-\frac{\delta_{ij}}{r^2}+\frac{2x_ix_j}{r^4}\right) ,$$

where the strength of the source doublet $\boldsymbol{D}$ depends on the problem geometry (location of the Stokeslet and distance between walls). On the other hand, a Stokeslet directed normal to the plane walls has a far field velocity that vanishes exponentially.

Exercise 12.3 Properties of the Lorentz and Mirror Reflection Operations.
Show that the Lorentz and mirror reflection operations commute, *i.e.*, $\mathcal{M}(\widehat{\boldsymbol{v}}) = \widehat{\boldsymbol{u}}$ where $\boldsymbol{u} = \mathcal{M}(\boldsymbol{v})$. Show that if $\boldsymbol{v}$ is satisfies the Stokes equations, then $\widehat{\boldsymbol{v}}$ is also a solution.

Exercise 12.4 A Consequence of the Lorentz Reciprocal Theorem.
Let $\boldsymbol{v}^F$ be the image of the Stokeslet field, $\boldsymbol{F}^{ext}\cdot\mathcal{G}(\boldsymbol{x}-\boldsymbol{y})$, and let $\boldsymbol{v}^Q$ be the image of the Stokes quadrupole field, $\boldsymbol{F}^{ext}\cdot\nabla^2\mathcal{G}(\boldsymbol{x}-\boldsymbol{y})$. Use the Lorentz reciprocal theorem to prove that

$$\nabla^2\boldsymbol{v}^F(\boldsymbol{x})|_{x=y} = \boldsymbol{v}^Q(\boldsymbol{y}) .$$

The extension of this result to the image fields of a viscous drop is given in Fuentes *et al.* [17].

Exercise 12.5 Image of a Rotlet Near a Rigid Plane Wall.
Derive the image for a rotlet near a plane wall. For the axisymmetric rotlet with $\boldsymbol{T}^{ext} \parallel \boldsymbol{n}$, what is the nature of the image singularity?

Exercise 12.6 A Spherical Drop Translating Near a Fluid-Fluid Interface.
Generalize Example 12.1 to obtain the translational mobility of a small spherical drop moving near a planar fluid-fluid interface. Compare your result with that obtain from the two-sphere problem of Chapter 10 in the limit of small h/a [16, 17].

Exercise 12.7 Force Balance on the Fluid-Fluid Interface.
Consider a fluid-fluid interface (placed on the plane $z = 0$) with large surface tension γ. Examine σ_{33} for a Stokeslet plus its image and estimate the amount of deformation of the interface [47]. Consider both axisymmetric and transverse Stokeslets.

Exercise 12.8 Computer-Aided Method of Reflections for a Sphere Near a Plane.
Consider a sphere of radius b near a plane wall. By combining the Lorentz reflection principle and the addition theorems for the spherical harmonics, as in Jeffrey and Onishi [38], derive a recursion scheme to generate the series solution in b/h to high orders. Compare your results with the solutions obtained by separation of variables in bispherical coordinates [4, 22].